APPLICATION OF ALOS DATA IN STUDYING ALPINE GLACIERS IN THE MT. HIMALAYAS ON THE TIBETAN PLATEAU

PI No.**411**

Qinghua YE[1,2], Jiancheng Shi[2], Xiao Cheng[3], Xin Li[4], Volker Hochschild[5]

[1] Key Laboratory of Tibetan Environment Changes and Land Surface Processes, Institute of Tibetan Plateau Research, Chinese Academy of Sciences (CAS), Beijing 100085, China,
Address: 18 Shuangqing Road, Haidian District, P.O.BOX 2871, Beijing 100085, China
Tel：+86 10 62849397, Fax：+86 10 62849886, E-mail: yeqh@itpcas.ac.cn

[2] State Key Laboratory of Remote Sensing Science, Institute of Remote Sensing Applications, CAS, Beijing 100101, China

[3] College Of Global Change and Earth System Science, Beijing Normal University, Beijing 100875, China

[4] Cold and Arid Regions Enviromental and Engineering Research Institute, CAS, Lanzhou 730000, China

[5] Physische Geographie und GIS, Geographisches Institut, Universitaet Tuebingen, 72070 Tuebingen, Germany

ABSTRACT

We studied alpine glacier variations (include change of ice volume by high resolution DEMs using PRISM stereo pair) glacier and ice volume variations at the margin of the Tibetan Plateau in China, e.g., in the Mt. Naimona'Nyi (the highest peak of the southwestern Himalayan Mountains, with an elevation of 7694 m a.s.l.), or the north slope of Mt. Everest region in Tibetan Plateau in the last 30 years using a series of multi-various digital satellite image data since 1970s (including ALOS/PRISM and ALOS/AVNIR-2 image data).

Glacier advance exits in some region, while glacier retreat dominates. Most of the glacier retreat area occurs at the termini of glaciers in the southeastern slopes of the two regions, whereas most of the glacier advance area occurs at the termini of glaciers in the northwestern slopes.

In addition to the popular methods by comparing individual images, we also integrated all classification results from various individual images by the algebraic operations in GIS which enables us to determine mismatched information, unreasonable changes in glacier variations, and evaluate ALOS image data measurement accuracy. The results obtained using both the "individual image" and the "integrated" method are presented in the program report.

The application of ALOS data in the Mt. Naimona'Nyi on Tibet glacier monitoring were carried out and its primary results were presented in this interim report.

Keywords: ALOS, alpine glaciers, Mt. Naimona'Nyi, Mt. Himalayas, Tibetan Plateau.

1. INTRODUCTION

Glacier variations on Tibetan Plateau play an important role in the global climate system, hydrological cycling and water resources. The successful launch of ALOS (with PRISM, AVNIR-2, and PALSAR instruments) provides a new prospect on monitoring of glacier changes on the Tibetan Plateau.

1.1 Research objectives

Our research goal in this project is listed in the followings:

- Evaluation of the ALOS/AVNIR-2 imagery in glacier studies on Tibet (Compared with other data by remote sensing and ground observation)
- Generation and accuracy of high resolution DEMs using ALOS/PRISM stereo pair
- Feasible usage of ALOS/PRISM and ASTER for alpine glacier volume variations in Tibetan Plateau using multi-source DEM Data

1.2 Research implementation

Based on our previous researches on glacier variations in Mt. Naimona'Nyi region (the highest peak of the south-western Himalayan Mountains, 81°E–81°47'E; 30°04'N–31°16'N) and northern Mt. Qomolangma (also known as the Mt. Everest, located in the middle Himalayan Mountains, 27°59-28°11´N and 86°44´-86°59´E) by satellite images[1], we know that the glacier recessions in the Himalayan regions are dramatic [2]. According to it, our research within the ALOS RA2 program was carried out and it could be summarized in the following: ALOS data were ordered from JAXA/EORC/ALOS[1] in the research scope on the Tibetan Plateau since the beginning of the RA2 program in 2007. ALOS/AVNIR-2 data was used in studying glacier coverage change on Tibet based on the previous research[3]. Both 1A and 1B1 or 1B2 products of ALOS/AVNIR-2 products are tried in the research. We found that there were many lines on the images at 1A data level, after orthorectification the lines at glacier terminus were distorted, which could greatly affect the glacier delineation at the terminus (See detail in our interim report). In the 2007 PI symposium in Kyoto in November, Dr. Takeo Tadono suggested us using data at 1B1 or 1B2 level. Yes, the othoimages of 1B2 are smooth and good in glacier coverage study on Tibet.

ALOS/PRISM stereo pairs were used in Digital Elevation Model (DEM) generation for studying glacier surface elevation changes in the Himalayan Mountains. The major problem was that there were some holes (i.e., failure value) in the generated DEMs from ALOS/PRISM in the Mt. Himalayas. The holes were reduced to the maximum extent by adjusting the parameters and improving GCPs and TPs in the DEM generation. The measurement accuracy of ALOS data and its DEMs were evaluated by the base reference data, such as local topographic maps in 1970s and its DEMs.

Table 1. Digital satellite images used in the Mt. Naimona'Nyi and Mt. Qomolangma region

Region	Sensor	Date
Mt. Naimona'-Nyi region	Landsat2 MSS	19761206
	Landsat5 TM	19901023
	Landsat7 TM	19991109
	Terra ASTER	20031003
	ALOS/AVNIR-2	20070909
	ALOS/PRISM	20060906
Mt. Qomolan-gma region	Landsat2 MSS	19761219
	Landsat5 TM	19921111
	Landsat7 ETM+	20001030
	Terra ASTER	20031023
	ALOS/AVNIR-2	20081024
	ALOS/PRISM	20061204

The SRTM DEM in the Mt. Qomolangma area was downloaded at http://srtm.csi.cgiar.org. The data is in Geotiff format, in decimal degrees and datum WGS84. They are derived from the USGS/NASA SRTM data. CIAT have processed this data to provide seamless continuous topography surfaces. Areas with regions of no data in the original SRTM data have been filled using interpolation methods described by Reuter et al. (2007) and Jarvis et al. (2008).

The Version 1 of the Advanced Spaceborne Thermal

[1] https://auig.eoc.jaxa.jp/auigs/top/TOP1000Init.do

Emission and Reflection Radiometer (ASTER) Global Digital Elevation Model (GDEM) was jointly released by METI of Japan and NASA on 29 June, 2009. Consequently, the ASTER GDEM is available at no charge to users worldwide via electronic download from the Earth Remote Sensing Data Analysis Center (ERSDAC) of Japan[1] and from LP DAAC[2].

The projection, datum and geoids of the download SRTM DEM and ASTER GDEM were transformed into the same projection reference system with the base topographic maps and DEM5. The height accuracy of SRTM DEM and ASTER GDEM were also evaluated by comparing 211 elevation check points on the 1:50,000 topographic maps with the corresponding height values for the same locations in the DEMs (Fig.1). We obtained an average height difference of 31.3 m and 44.9 m, with a standard deviation of 85.6 m and 77.7 m, respectively.

Fig.1 Distribution of 211 evaluation points in the non-glacierized area

Field survey on Tibet was also carried out in Sep.-Oct. in 2007, April-May, Aug., and Sep. in 2008, April, May, Aug., and Sep. in 2009, Sep. and Oct. in 2010.

2. METHODS

2.1. Glacier coverage monitoring by ALOS/AVNIR-2

Glacier coverage change was studied in the Mt. Himalayas both in the Mt. Naimona'Nyi and in the Mt. Qomolangma region in 1974-2008. Multi-sources of data were used, which included a series of digital images (Table 1), 1:50,000 topographic maps produced from aerial photographs acquired in 1974 with the Transverse Mercator projection and the Krasovsky1940 spheroid that was surveyed and mapped by State Bureau of Surveying and Mapping in China and its 1:50,000 Digital Elevation Model (DEM) with equidistant contour lines of 20 m and a cell size of 25 m (DEM5), topographic maps and the DEM5 were used as the common base in the research.

The raw digital satellite images (e.g. ASTER, ALOS/AVNIR-2) have been accurately orthorectified using the base DEM. The horizontal accuracy of the DEM5 with respect to the 1:50,000 topographic map of the region is within 1.0 grid cell, i.e., 25 m. The height accuracy of the DEM was also evaluated by 331 and 344 elevation check points on the 1:50,000 topographic maps with an average height difference of 12.37 m [1] and 13.3 m [3] in the Mt. Naimona'Nyi and Qomolangma region, respectively. The accuracy of ortho-rectification was within one image pixel. Precise co-registration for all ortho-images was based on the 1:50,000 topographic maps, all co-registration errors being within one image pixel.

To improve the contrast between the glacier ice and surrounding areas, false color composite images were constructed using bands 4, 2, and 1 (i.e. RGB: 421)from Landsat MSS, bands 4, 3, and 2 (RGB: 432) from the Landsat TM or ETM+, bands 3N, 2, and 1 (RGB: 3N21) from the ASTER, and bands 4 (0.76-0.89 μm), 3 (0.61-0.69 μm), and 2 (0.52-0.60 μm) (RGB: 432) from ALOS/AVNIR-2. Glaciers from ALOS/AVNIR-2 image were classified by unsupervised classification using false color composites in Mt. Naimona'Nyi region, whereas cloud-covered non-glacierized areas were removed by manual editing (Fig. 2). Glacier classifications from other images in Mt. Naimona'Nyi study region follows the methods described by Ye and others[1]. In the Mt. Qomolangma area, the Landsat MSS in 1976 was not used because of the big mountain shade in the image. Glaciers with terminus at seracs on the 1:50,000 scale topographic maps and sequential Landsat images were mapped in the false color image by on-screen digitizing with manual delineation in the Arc/Info software. The accuracy of manual digitization was controlled within one pixel [3].

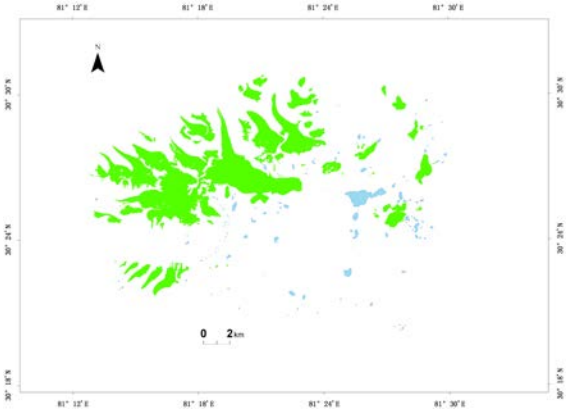

Fig. 2 Glaciers and lakes in Mt. Naimona'Nyi region from ALOS/AVNIR-2 on Sep. 6th in 2007

[1] http://www.gdem.aster.ersdac.or.jp/
[2] https://wist.echo.nasa.gov/~wist/api/imswelcome/

Fig. 3 ALOS/AVNIR-2 (RGB: 432) image on Oct. 24th in 2008 in the Mt. Qomolangma region

Based on the usual method for studying glacier change, we developed a multi-temporal grid method for studying glacier variations by means of GIS and Remote Sensing techniques. We used 30 m grid-cell as the basic unit, i.e., all glacier classification results from individual images were re-sampled to the same pixel size by 30 m grid cell resolution. Discrete grid cells of a fixed resolution are suitable for spatial and temporal analysis of large quantities of data in GIS. We consider a variable of $P_i(x,y)$ that expresses the attribute feature P_i, i = 1,..,*m*, at sampling time T_k and spatial position $S_k(x_k, y_k)$ for $k = 1,\ldots,n$. Synthesized by map algebra in the Arc/Info Grid module [4], the multi-temporal grid unit has all the sequential attribute information of glaciers within the study area. It is a synthesis of glacier characteristics of "space· attribute· process" and is fundamental to providing insights into spatial and temporal dynamics of transition sequences. The unit in the series of multi-temporal grids is similar to the geographic unit, which could also be classified into a series of multi-categories at multi-grades and multi-scales[4].

The multi-temporal grid enabled us to track spatial-temporal changes of glaciers in each grid cell during the corresponding period. Various types of glacier variation occur in the original synthesized data[4]. We therefore developed a methodology to understand the principal changes. We analyzed the different types and reclassifications of the grid cells according to the several-digit value in order to identify glacier retreat and advance areas. The four or five digit value from each multi-temporal grid cell was used to differentiate between real glacier changes during the observation period and noise, caused by geolocation error (e.g. systematic error) or misclassifications (i.e. noise). The major affiliation principles were also applied in detection and elimination of some noises. The primary principles for distinguish real glacier changes were based on characteristics of glacier dynamics[4].

2.2. DEM generation from stereo pairs of ALOS/PRISM

Calculation on glacier volume variations are still greatly limited by the vertical accurate of various data sources till now[5]. Therefore, one of the major methodological gaps in the observation of glaciers from space is the measurement of glacier volume changes [6]. Glacier volume changes needs an integrated study and correction on generated DEMs from multi-sources remote sensing data and evaluation of the vertical errors and accuracy. Here, the report introduced the process of DEMs generation over mountain glaciers from ALOS/PRISM on the northern slope of Mt. Qomolangma.

Digital Elevation Models (DEMs) were generated using the three stereo pairs from ALOS/PRISM on 04 Dec 2006 in PCI Orthoengine module software by various Algorithms. All of the three stereo pairs of ALOS/PRISM data were used together in the DEM generation process.

- Input the forward、backward、nadir digital images to the Orthoengine module of PCI Geomatica 9.2, the parameters of data importing were verified by Dr. Takeo Tadono in JAXA and summarized in Table 1.
- Define the project information, which was the same reference system as the base topographic maps and DEM5, i.e., Trans-Mercator projection and Krasovsky1940 spheroid.
- Choose Ground Control Points (GCPs) and Tie Points (TPs) based on the 1:50000 topographic maps and the DEM5. It is very difficult to choose the reference points because of high elevation and complex mountain topography. High quality of points was selected at crossings along the range, peaks, rocks and rivers at different altitude, including 29 GCPs and 12 TPs.
- Create Epipolar images and generate DEMs based on the stereo pair selection of three scenes from PRISM images in the PCI Orthoengine module.

Table1 The parameters of importing ALOS/PRISM into PCI software

	Backward	Nadir	Forward
Across angle	1.09	1.2	1.09
Along angle	-23.8	0	23.8
Altitude	691650m		
IFOV	0.00000361		
Semi-minor	6356752 m		
Inclination	98.176		
Ellipsoid	GRS80		
Period	98.7min		

As there are some holes (i.e. no value pixels, or areas with failure value) in the generated PRISM DEMs, algorithms of generating DEMs were adjusted from time to time in the process. For example, when the left image was forward data, the right image would use the nadir one, while the left image was the nadir data, the right image should be the backward data.

According to the limited pixel size of the base DEM, DEM5 (pixel size, 25 m), the output resolution of the generated DEM was also using the same resolution. However, there

are lots of holes (i.e. areas without value) in the generated PRISM DEM by 25 m. Those holes were minimized not only by the output resolution but also by adjusting the pixel sampling interval in the Epipolar DEM Extraction options. At the same time, the output pixel resolution was kept as fine as possible. There is a compromise between the minimum area of failure value and the pixel interval with fine resolution. Algorithms for the best compromise between the minimum area of failure value and the fine pixel size were accepted.

Various DEM products were obtained, e.g. by 1 pixel sampling interval (pixel resolution: 2.5m) with an output resolution of 25m(PRISM_25m_1p, Fig.4), By 2 pixel sampling interval with an output resolution of 25m(PRISM_25m_2p, Fig.5), 50m (PRISM_50m_2p, Fig.6), and 100m (PRISM_100m, Fig.7), by 4 pixel sampling interval with an output resolution of 50m(PRISM_50m_4p, Fig.8), etc.

2.3. DEM evaluation

2.3.1. Evaluation by Random Check Points in the non-glacierized area

The accuracy of the various DEM products was evaluated by 211 elevation check points in the non-glacierized area on the base 1:50,000 topographic maps. In statistics, it learns that while increasing the output pixel size, both the range of vertical deviations and the areas of holes were reduced. For example, PRISM DEM with an output resolution of 100m (PRISM 100m) is almost no holes (Fig.4) with smaller vertical deviation among all other generated DEMs. While using the same output resolution 50m, the 4 pixel sampling interval (resolution: 10m) scheme resulted in a larger area of failure value at high altitude (PRISM_50m_4p, Fig.5) than that of 2 pixels interval scheme (PRISM_50m_2p, Fig.6). By using the 1 pixel sampling interval (resolution: 2.5m) scheme, there is not an obvious difference in the area of failure value. However, a larger vertical deviation was also obtained that ranged from -289.0 m and 303.0 m in statistics (PRISM_25m_1p, Fig.4).

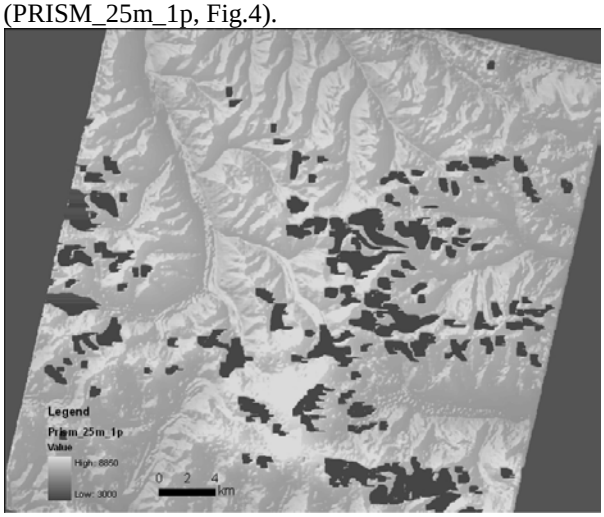

Fig.4 the generated PRISM DEM with an output resolution of 25m by 1 pixel sampling interval(PRISM_25m_1p)

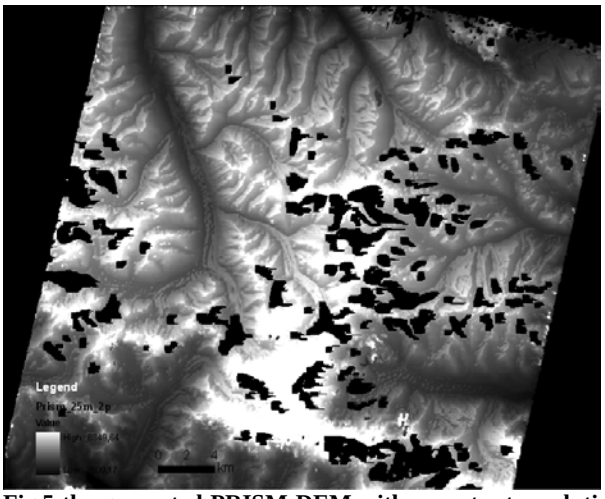

Fig.5 the generated PRISM DEM with an output resolution of 25m by 2 pixel sampling interval (PRISM_25_2p)

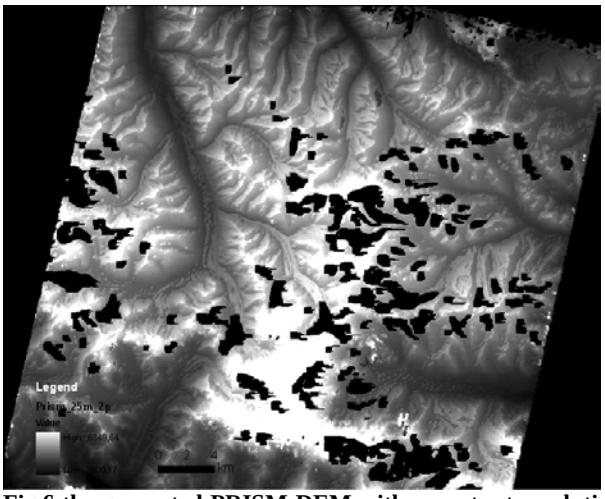

Fig.6 the generated PRISM DEM with an output resolution of 50m by 2 pixel sampling interval (PRISM_50m_2p)

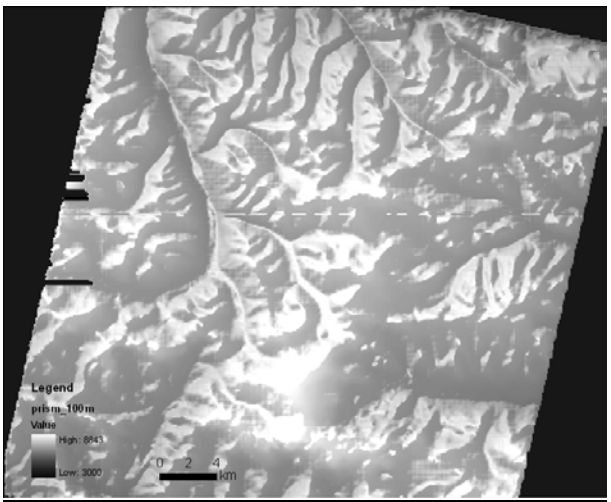

Fig.7 the generated PRISM DEM with an output resolution of 100m (PRISM 100m) by hill shade effects

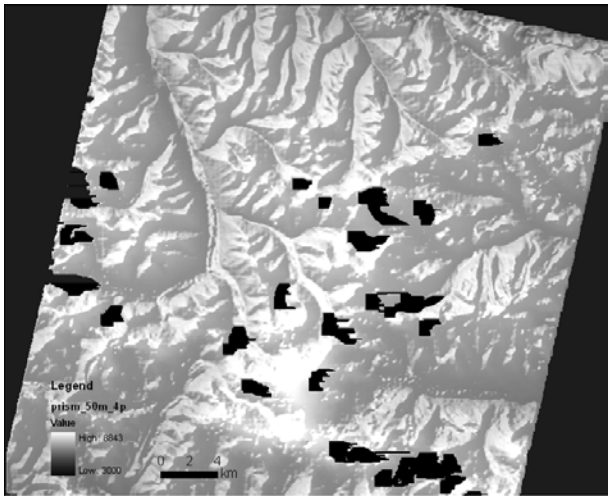

Fig.8 the generated PRISM DEM with an output resolution of 50m by 4 pixel sampling interval (PRISM_50m_4p)

It shows that the best result was obtained by 2 pixel sampling interval scheme with an output resolution of 25m (PRISM_25_2p, Fig.8), the mean difference is 4.1 m, with a standard deviation of 52.0 m, and the maximum height deviations ranged from -294.0 to 258.0 m.

2.3.2. Bias to the base DEM in the non-glacierized area

Comparing to the 1：50,000 base DEM (DEM5) in 1974, the mean difference of the PRISM_25m_2p DEM was 2.5 m, with a standard deviation of 102.6 m, and maximum height deviations ranged from -2019.8 to 3303.6 m. The mean difference of the PRISM_25m_1p DEM is 0.07 m, with a standard deviation of 103.6 m, and maximum height deviations ranged from -1874.9 to 3369.0 m. While the mean difference of the PRISM_100m DEM is 1.93 m, with a standard deviation of 92.4 m, and maximum height deviations ranged from -523.1 to 3305.0 m.

As to the available DEM products by comparing to the 1：50,000 base DEM (DEM5), the mean difference of the SRTM DEM was 11.3 m, with a standard deviation of 77.1 m, and maximum height deviations ranged from -323.0 to 412.2 m. While the mean difference of the ASTER_GDEM is 28.7 m, with a standard deviation of 79.4 m, and maximum height deviations ranged from -263.3 to 1040.3 m.

2.3.3 DEM calibration and validation

Before the generated PRISM DEMs are used to calculate glacier volume changes, the differences/offsets in the non-glacierized area between the generated DEMs and DEM5 were carefully analyzed according to different topography factors, which include altitude, slope and aspect. From the 2D scatter dots figures between DEMs difference and topography factors, we found that there are close relationships between DEM offsets and the altitude, slope and aspect. The range of offsets could be very large due to different spatial and topography factors.

By Spatial Analyst Tools in Arc/GIS, zonal statistics were carried out for offsets in the non-glacierized area between the generated PRISM DEM and the base DEM5 in different altitude by 20 m interval, each zone in 8 aspects and different slopes. Relationships between offsets and various topographic factors (e.g. altitude, slopes and aspects) in space were set up using linear or multi poly formulas. Close relationships between offsets and aspects was selected as the calibration formula (Fig.9).

Non-glacierized areas in the generated DEM were calibrated according to the formula in Fig.9. The calibrated part of **PRISM_25_2p** DEM in non-glacierized areas was re-evaluated by the base topographic maps and DEM5. However, the average difference between calibrated DEM and the reference DEM was 2.79 m (Fig.10), which was even larger than the original generated one, it might because some other bias/errors was induced into the calibrated DEM.

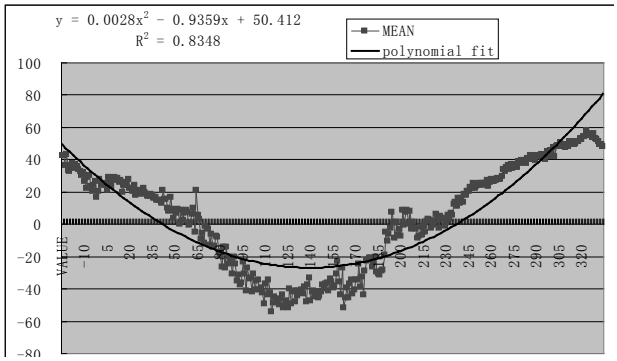

Fig.9. Relationship offsets and aspects for ALOS PRISM DEM (PRISM_25_2p)

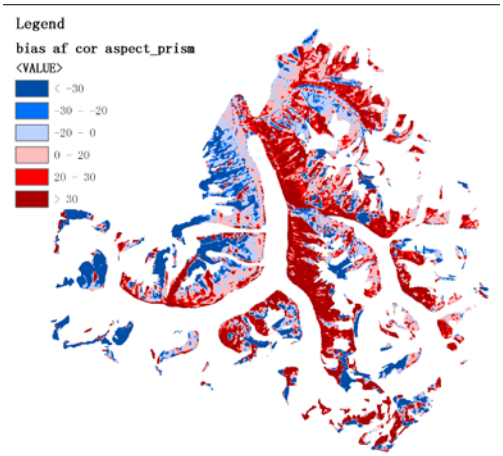

Fig. 10 Corrected PRISM DEM(PRISM_25_2p_correct)

Therefore, careful check and calibration work needs to be carried out further for the **PRISM_25_2p**. Those holes in the originally generated ALOS/PRISM DEM (PRISM_25m_2p) was filled by SRTM DEM and now used in the glacier vertical changes in the report.

3. RESULTS

3.1. Glacier coverage change

3.1.1 In the Mt. Qomolangma region

The glacier area in the study region, was 144.14 km^2 in 1974 and decreased to 129.13 km^2 in 2008, the glacier recession being equal 15.01 km^2, i.e. 10.41% or 0.30 % a^{-1}, 0.43 km^2 a^{-1} in the last 35 years. There are 74 glacier segments in 1974, 13 segments being larger than 1 km^2 (totaling 125.46 km^2 and occupying 87.04% of the total glacier area), 15 segments between 0.5 km^2 and 1 km^2 (10.15 km^2, or 7%), and 46 segments smaller than 0.5 km^2 (8.53 km^2, or 5.92%). The rates of change vary for different size of glaciers in different periods. Smaller glaciers were more sensitive to changes than the larger ones. During 1974-2008, glaciers that smaller than 1 km^2 were lost 14.96% (2.79 km^2, or 0.43% a^{-1}), whereas larger glaciers retreated by 9.74% (12.22 km^2, or 0.28% a^{-1}). Among them, the Rongbuk glacier, with three branches that totals to 93 km^2 in 1974 retreated with 10.54% (9.8 km^2, or 0.30% a^{-1}). Three small glaciers, with area of 0.03 km^2, 0.02 km^2 and 0.03 km^2 in 1974, disappeared totally before 1992 [3].

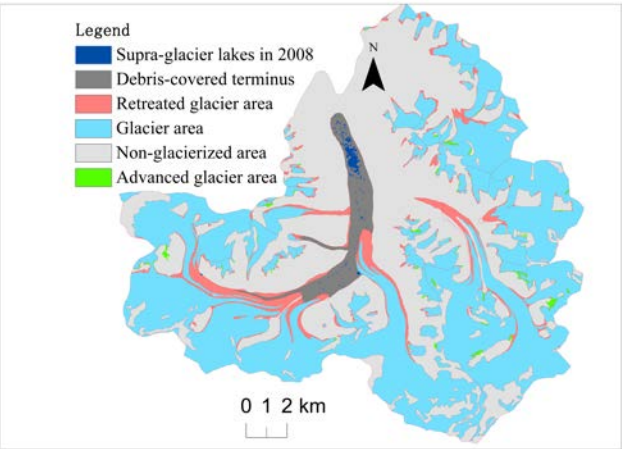

Fig. 11 Glacier variations in Mt. Qomolangma region during 1974–2008

There were some advanced glacier areas, which totals to 1.29 km^2 in 1974-2008(Fig. 11).

Glacier change in the study region also shows spatial differences during 1974-2003. Glacier terminus was located at approximately 5400 m a.s.l. in the region. At glacier termini between 5400 and 5700 m a.s.l, glacier retreat rate was fastest (more than 51% of the total area by 8.15 km^2) than at other elevations. For glacier termini areas at a higher altitude, glaciers had a lower recession rate. On the Mountain top, no glacier recession was observed.

3.1.2 In the Mt. Naimona'Nyi area

The total glacier coverage was 86.03 km^2 in 1976 and decreased to 75.62 km^2 in 2007. There are 79 glacier segments in the region from the 1:50,000 topographic maps in 1974, 21 segments being larger than 1 km^2 (totaling 70.60 km^2 and occupying 79.33% of the glacier area), 13 segments between 0.5 km^2 and 1 km^2 (10.0 km^2, or 11.23%), and 45 segments smaller than 0.5 km^2 (8.39 km^2, or 9.43%), which reduced to 41 segments in 2007. In 1976-2007, there are 4 small glaciers segments disappeared, with coverage sizes equal to 0.29 km^2, 0.02 km^2, 0.02 km^2 and 0.01 km^2 in 1976. The rate of glacier change was different by different sizes in different periods. Smaller glaciers were more sensitive to change than larger ones. For the glacier segments of the small size, whose coverage area was less than 0.5 km^2, advance and retreat were more rapid than larger ones. Both advance and retreat co-exist and retreat dominates in 1976-2007 (Ye et al., in preparation).

For glaciers that smaller than 1 km^2, the total coverage was equal to 15.70 km^2 in 1976 and decreased to 13.34 km^2 in 2007, its total recession being 15.00% or 0.47% a^{-1} in 1976-2007. It obviously seems that glacier retreat was accelerated. However, glaciers coverage had increased by 0.67 km^2, 5.27% or 1.05% a^{-1} in 2003-2007. Coverage advance of smaller glaciers (< 1 km^2) was more obvious since 2003. For all glaciers smaller than 1 km^2, both advance and retreat were more rapid than larger ones and their variation trends were similar by the two different sizes (Fig.12).

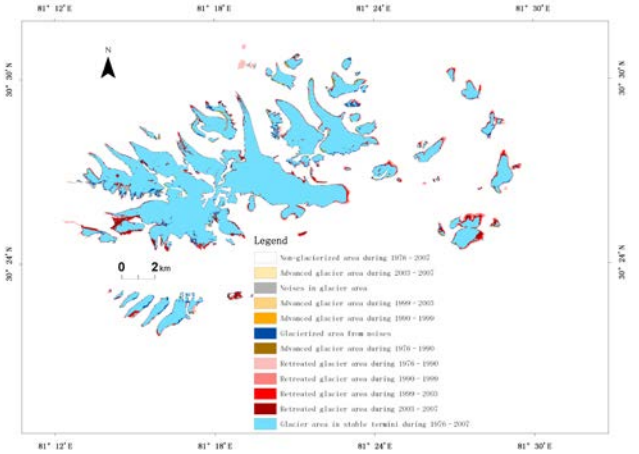

Fig. 12 Glacier coverage variations in the Mt. Naimona'Nyi region during 1976–2007

For glaciers larger than 1 km^2, the total glacier recession between 1976 and 2007 was 5.09 km^2, 7.66% or 0.24 % a^{-1}. Glacier recession was 0.17 km^2 during 1976–1990 (0.01 km^2 a^{-1} or 0.02 % a^{-1}), 1.17 km^2 during 1990–1999 (0.12 km^2 a^{-1} or 0.18 % a^{-1}), 1.87 km^2 during 1999–2003 (0.37 km^2 a^{-1} or 0.57 % a^{-1}), and 1.88 km^2 during 2003–2007 (0.38 km^2 a^{-1} or 0.59 % a^{-1}). The largest glacier segment covered by 8.16 km^2 in 1976 and decreased to 7.78 km^2 in 2007, its recession being 4.62% or 0.14% a^{-1}. In Table 3, a clearly accelerated glacier recession in 1976-2003 was presented. In 1976-2007, there was a north facing glacier which was advanced in 1976-1990 and retreated since then, with an area by 4.87 km^2 in 1976, increased to 4.94 km^2 (i.e. increased by 0.01 km^2 a^{-1}, 1.59% or 0.11 % a^{-1}) in 1990, then decreased to 4.92 km^2 in 1999 (i.e. decreased by 0.003 km^2 a^{-1} or 0.05 % a^{-1}), 4.80 km^2 (i.e. decreased by 0.02 km^2 a^{-1} or 0.48 % a^{-1}) in 2003, and 4.70 km^2 (i.e. decreased by 0.02 km^2 a^{-1} or 0.42 % a^{-1}) in 2007, respectively.

In a word, it shows that both glaciers advancing and

retreating were increased in 2003-2007.

Glacier variations in Mt. Naimona'Nyi region also show spatial differences during 1976-2007. Glaciers located on slopes between 20° and 25° retreated more dramatically (recession was about 18.55%) than glaciers at other slopes. At glacier terminus between 5400-5700 a.s.l, glaciers retreat rate was the fastest (around 50% of the total area by 5 km^2) than other elevations, the second rate (more than 19.75% recession) locates between 5700-6000 a.s.l. In different aspects, glaciers located in east, southeast aspects retreated fastest (recession was above 16%), glaciers on the flat (recession was above 14.78%) also retreated more dramatically than those glaciers in other aspects. In our statistics above, the majority and median glacier size on different slopes, aspects and altitude were larger than 1 km^2, while the minority glaciers were all smaller than 1 km^2.

3.2. Vertical change on glacier surface

On the glaciers in the Mt. Qomolangma region, vertical changes in 1974-2006 showed obviously different in space (Fig.13). It showed that in the last 33 years, areas of negative value, i.e. areas with surface increasing in Fig.13, usually locate at the accumulation zones of the glaciers. It seems that the dramatic melting zones with downwasting of 60 m locate at glaciers terminus.

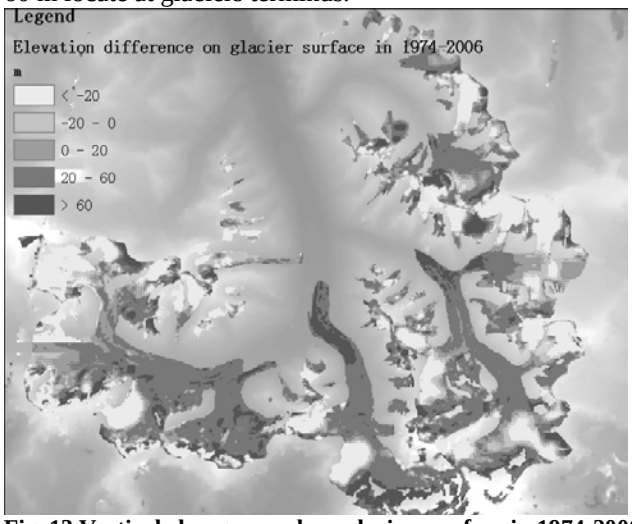

Fig. 13 Vertical changes on clean glaciers surface in 1974-2006

By altitude in every 20 m interval, vertical changes on glacier surface were averaged and presented in Fig.14. It showed that in the last 33 years, glacier termini were the dramatic melting zones, where average annual downwasting was above 2 m.

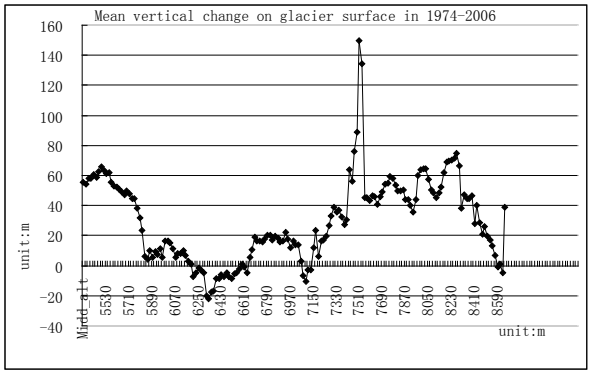

Fig.14 Average vertical changes on glacier surface by altitude in every 20 m interval

On the debris covered part of Rongbu Glacier, by the mean change in every 20 m interval in altitude, it shows that the most downwasting part located between 5310 m and 5330 m at the terminus, which was more than 60 m during 1974-2006. The most remote downwasting part locates at 5250 m, which lost 50 m in the last 33 years. It might be the glacier terminus of Rongbu with debris cover in 1974.

In lakes on the debris covered terminus of Rongbu Glacier, the mean vertical downwasting change was 43.15 m, the Standard deviation was 20.07, with the minimum -65.72 m and maximum 107.85 m. In Fig.15, it shows an obvious spatial difference on vertical changes in lakes. The closer to the glacier ices, the thicker lose existed. The most remote downwasting part locates at 5270 m, which lost more than 60 m in the last 33 years. It might because of the terminus retreating of the Rongbu glacier since 1974.

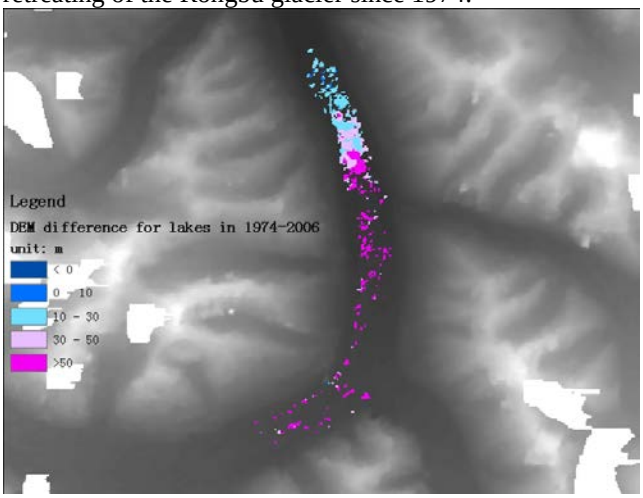

Fig. 15 Vertical changes in lakes on debris-covered terminus in 1974-2006

4. DISCUSSION

The measurement accuracy of the position of the glacier front by remote sensing satellite images is limited by both the sensor resolution [7] and the coregistration error[8, 9]. Calculated by the sensor resolution and coregistration error[2], the maximum measurement uncertainty in area extent of glaciers was approximately 0.015 km^2 in the Mt. Naimona'Nyi region, 0.044 km^2 in the Mt. Qomolangma area, and 0.042 km^2 in Mt. Geladandong area. Using the

multi-temporal grid method, however, we eliminated more than 2.5 km^2 of noise or 3.0% of the total glacier area in 1976 from classification results in the Mt. Naimona'Nyi region. Similarly, corrections of approximately 11 km^2 of noise or 1.2% of the total glacier area in 1969 was made for the Mt. Geladandong area. Such noise among sequential data sets was much higher than that of the measurement uncertainty by sensor resolution and coregistration error. Therefore, uncertainty in glacier monitoring by satellite images mainly originates from such noise in sequential data sets, caused by geolocation error or misclassifications.

In Mt. Qomolangma area DEM was also generated using two stereo pairs from ASTER images on 23 Oct 2003 in PCI Orthoengine module software. The process of DEM generation from ASTER images is very similar to that of ALOS/PRISM (Fig.16). The difference is that: only two images from nadir and backward views were used for ASTER DEM. However, comparing to the base DEM, its mean offset was 41.7 m, which was higher than the generated ALOS/PRISM DEM. Therefore, ALOS/PRISM data is more accurate than ASTER stereo pairs in DEM generation because of its high pixel resolution.

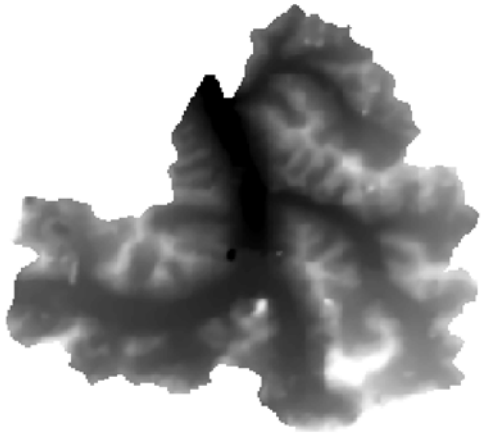

Fig.16 the generated ASTER DEM on 23 Oct 2003

In the Mt. Naimona'Nyi region, Dr. Takeo Tadono has helped us in DEM generation using the three stereo pairs from ALOS/PRISM on Sep.6 in 2006. The holes are filled by SRTM DEM. However, the generated DEM is still not being opened and evaluated, further efforts needs to put for it before usage.

5. CONCLUSION

Glaciers in this region have both retreated and advanced during the last several decades in the warming climate, with retreat dominating and accelerating. Glacier coverage change is analyzed both by glacier sizes and by different spatial features, e.g. different elevations, slopes and aspect. For smaller glaciers that were smaller than 1 km^2, both glacier coverage and its advance rate were increased obviously in 2003-2007, which might due to the increased precipitation, glacier surge or accelerated hydrological process in the warming climate. It shows that glaciers retreat extensively in the Himalayas.

It presents that the quality of the generated ALOS/PRISM DEM by 25 m pixel resolution (prism_25m_2p) is a more accurate one to DEM5. It is better than other generated and download DEM products.

The DEMs need to be evaluated or calibrated before their usage. However, sometimes the average difference between calibrated DEM and the reference DEM was even larger than the original generated one, it might because some other bias/errors was induced into the calibrated DEM. Therefore, the generated and calibrated ALOS/PRISM DEM was also need to be further analyzed or evaluated by the base DEM.

In a word, ALOS data is very good at glacier monitoring researches because of its advantages in high spatial resolutions.

6. ACKNOWLEDGEMENT

The research results have been obtained through the cooperation between the research organization (Institute of Tibetan Plateau Research, CAS) and JAXA(JAXA/METI for PALSAR) in JAXA's ALOS RA. The authors would like to thank Dr. Takeo Tadono, who provides lots of suggestions and help in data processing. The work is also supported by the Special Funds for Major State Basic Research Project (2009CB723901), by the National Natural Science Foundation of China (40971048,40601056), by the Opening Fund projects of State Key Laboratory of Remote Sensing Science in the Institute of Remote Sensing Applications, by the Innovation Foundation Project for outstanding Young Scientist of CAS (Grant No. KZCX2-EW-QN104).

7. REFERENCES

[1] Q. Ye, *et al.*, "Glacier variations in the Naimona'nyi region,western Himalaya, in the last three decades," *Annals of Glaciology*, vol. 43, pp. 385-389, 2006.

[2] Q. H. Ye, *et al.*, "Monitoring Glacier Variations on Geladandong Mountain, Central Tibetan Plateau, from 1969 to 2002 Using Remote-Sensing and GIS Technologies. ," *Journal of Glaciology*, vol. 52, pp. 537-545, 2006.

[3] Q. Ye, *et al.*, "Monitoring glacier and supra-glacier lakes from space in Mt. Qomolangma region of the Himalayas on the Tibetan Plateau in China," *Journal of Mountain Science*, vol. 6, pp. 101-106, 2009.

[4] Q. Ye, *et al.*, "Use of a multi-temporal grid method to analyze changes in glacier coverage in the Tibetan Plateau," *Progress in Natural Science*, vol. 19, pp. 861-872.*Enclosing as copies, 2009.

[5] N. F. Stevens, *et al.*, "NASA EOS Terra ASTER: Volcanic topographic mapping and capability," *Remote Sensing of Environment,* vol. 90, pp. 405-414, 2004.

[6] A. Kääb, "Glacier Volume Changes Using ASTER Satellite Stereo and ICESat GLAS Laser Altimetry. A Test Study on Edgeøya, Eastern Svalbard," *IEEE Transactions on Geosciences and Remote Sensing,* vol. 46, pp. 2823-2830, 2008 2008.

[7] R. S. Williams, Jr., *et al.*, "Comparisson of satellite-derived with ground-based measurements of the fluctuations of the margins of Vatnajökull, Iceland, 1973-1992," *Annals of Glaciology,* vol. 24, pp. 72-80, 1997.

[8] W. Silverio and J.-M. Jaquet, "Glacial cover mapping (1987-1996) of the Cordillera Blanca (Peru) using satellite imagery," *Remote Sensing of Environment,* vol. 95, pp. 342-350, 2005.

[9] D. K. Hall, *et al.*, "Consideration of the errors inherent in mapping historical glacier positions in Austria from the ground and space (1893-2001)," *Remote Sensing of Environment,* vol. 86, pp. 566-577, 2003.